Revista ALCONPAT
www.revistaalconpat.org
eISSN 2007-6835
Revista de la Asociación Latinoamericana de Control de Calidad, Patología y Recuperación de la Construcción

Corrosion sensor for monitoring reinforced concrete structures: Tests on reinforced concrete specimens

A. Calvo Valdés[1], M. H. F. Medeiros*[1], G. Macioski[1]
*Contact author: medeiros.ufpr@gmail.com
DOI: https://doi.org/10.21041/ra.v11i3.529

Reception: 19/01/2021 | Acceptance: 03/08/2021 | Publication: 01/09/2021

ABSTRACT

The aim of the research was to evaluate the effectiveness of a galvanic multi-electrode sensor to detect the probability of corrosion in reinforced concrete prisms subjected to drying and wetting cycles in a NaCl solution. The corrosion potential (E_{corr}) readings obtained using a copper sulfate copper electrode ($Cu/CuSO_4$) were analyzed along with the galvanic current (I_{gal}) and galvanic potential (E_{par}) readings. The sensor developed showed sensitivity to detect the chloride front and to predict the possibility of corrosion of the reinforcement. The parameters E_{corr}, E_{par} and I_{gal} presented distinct behaviors in terms of its use as parameters for corrosion monitoring.

Keywords: corrosion; potential; galvanic sensor; galvanic current.

Cite as: Calvo Valdés, A., Medeiros, M. H. F., Macioski, G. (2021), "*Corrosion sensor for monitoring reinforced concrete structures: Tests on reinforced concrete specimens*", Revista ALCONPAT, 11 (3), pp. 64 – 87, DOI: https://doi.org/10.21041/ra.v11i3.529

[1] Universidade Federal do Paraná, Rua XV de Novembro, 1299 - Centro, Curitiba - PR, 80060-000, Brasil.

Contribution of each author
In this work, the authors Analiet Calvo Valdés and Marcelo H. F. Medeiros contributed to the activities of bibliographic consultation, writing of the text and development of the experimental program, a total number of 33.3% each. Or author Gustavo Macioski with bibliographic review and consultation activity, completing the remaining 33.3%.

Discussions and subsequent corrections to the publication
Any dispute, including the replies of the authors, will be published in the second issue of 2022 provided that the information is received before the closing of the first issue of 2022.

Sensor de corrosão para monitoramento de estruturas de concreto armado: Testes em corpos de prova de concreto armado

RESUMO

O objetivo do trabalho foi avaliar a eficácia de um sensor galvânico de múltiplos eletrodos na detecção da probabilidade de corrosão em prismas armados de concreto submetidos a ciclos de secagem e molhagem em uma solução de NaCl. Se analisaram as leituras de potencial de corrosão (E_{corr}) obtidas por meio de um eletrodo de referência de cobre sulfato de cobre ($Cu/CuSO_4$) com as leituras de corrente galvânica (I_{gal}) e potencial galvânico (E_{par}). O sensor desenvolvido apresentou sensibilidade para detectar a frente de cloretos e prever a possibilidade de corrosão das armaduras. As grandezas E_{corr}, E_{par} e I_{gal} apresentaram comportamentos distintos como parâmetro de monitoramento da corrosão.

Palavras-chave: corrosão; potencial; sensor galvânico; corrente galvânica.

Sensor de corrosión para monitorear estructuras de hormigón armado: Ensayos en especímenes de hormigón armado

RESUMEN

El objetivo del trabajo fue evaluar la efectividad de un sensor galvánico multi-electrodo en la detección de la probabilidad de corrosión en prismas de hormigón armado sometidos a ciclos húmidos y secos en una solución de NaCl. Se analizaron lecturas de potencial de corrosión (E_{corr}), obtenidas utilizando un electrodo de cobre de sulfato de cobre ($Cu/CuSO_4$), lecturas de corriente galvánica (I_{gal}) y potencial galvánico (E_{par}). El sensor desarrollado mostró sensibilidad para detectar el frente de cloruro y predecir la posibilidad de corrosión de la armadura. Las variables E_{corr}, E_{par} e I_{gal} presentaron comportamientos diferentes como parámetros para monitorear la corrosión.

Palabras clave: corrosión; potencial; sensor galvánico; corriente galvánica.

1. INTRODUCTION

The degradation of concrete structures due to corrosion affects civil construction throughout the world, with repercussions depending on the volume of registered cases, the precocity with which they occur, and the amount of resources involved in their evaluation and repair (Meira, 2017).
The annual cost of corrosion worldwide exceeds 3% of the world's Gross Domestic Product (GDP), approximately USD 2.2 trillion (Hays, 2020). Depending on when the intervention is carried out, the costs can be compounded (Meira, 2017), and may even exceed the original cost of construction (Dong et al., 2011).
Corrosion reduces the yield strength of steel, weakens the bonding properties between reinforcement and concrete, and affects the seismic performance and static load capacity of reinforced concrete structures. Iron oxidation (with Fe_2O_3 as the main component) is produced by the corrosion of steel bars, which causes the expansion of volume and tensile stress in the concrete, and subsequently causes the concrete to deform and crack (Zhao et al., 2017).
Corrosion of the steel bar inside the concrete essentially occurs for two reasons: first, due to the reduction in the alkalinity of the concrete caused by carbonation, and second, due to the presence of chlorides, which even with high pH, depassivate the reinforcement causing an intense and localized attack (France, 2011).
Investigation of affected structures usually involves an assessment of their durability (Wu et al., 2017). Durability is the result of the interaction of concrete structures with the environment, and is influenced by conditions of use, operation and maintenance processes. To assess the performance of constructions, visual inspections associated with field and laboratory tests are used (Mota, 2011). Systematic visual inspections certainly reduce the level of uncertainty regarding the state of the structure, but this technique has important limitations, as it is based on superficial observations of the structure over short periods of time (Inaudi, 2009), which can result in dangerous errors and inefficient use of resources for the maintenance of the structures.
Through sensors, it is possible to obtain data on a regular basis, ensure simultaneous readings at different points and, consequently, make different measurements compatible (Santos, 2014). Sensors are able to provide real-time information (Zhao et al., 2017) that feeds mathematical models to predict life cycle (Araújo et al., 2013) in order to estimate two fundamental stages of the corrosion phenomenon: the initiation phase and the corrosion propagation phase, according to the phenomenological model proposed by Tuutti (1982) (Figueiredo and Meira, 2013).
In this way, it is possible to carry out forecasts of the monitored structures and reduce the costs associated with restoration or replacement work. In Brazil, for example, according to a study by the Institute for Applied Economic Research (IPEA), by the year 2025 just over 89 million Brazilian reais must be earmarked for the maintenance of 15 bridges in 12 states of the Federation. Part of this money will be invested in monitoring systems, since the use of sensors can provide greater durability and sustainability of public infrastructure works (M. Torres-Luque et al., 2014).
In the US, according to the Federal Highway Administration (FHWA), in accordance with a report by the American Society of Civil Engineers (ASCE) for the year 2013, 20.5 billion dollars a year must be invested by 2028 in the maintenance of public infrastructure works. In Europe, the estimated annual cost of maintenance on reinforced concrete bridges is around 1 billion euros (Zoghi, 2013).
Therefore, industrialized electrochemical sensors have attracted attention (Zhao et al., 2017), including: embedded electrodes, macro corrosion current probes, linear polarization sensors, electrical resistance sensors, corrosion potential sensors and galvanic sensors (Dong et al., 2011; Chen et al., 2017).
In the context of chloride corrosion induction, a galvanic sensor is probably the best option for monitoring (Klassen and Roberge, 2008). Its installation in the structure provides measurements of

galvanic current intensity and corrosion potential that allow monitoring the depth of the chloride penetration front (Mccarter and Vennesland, 2004; Andrade et al., 2008; Araújo et al., 2013). These sensors are formed by two metals with different electrical potentials (anode and cathode) (Andrade et al., 2008), spatially separated (Angst and Buchler, 2015).

The galvanic macrocell created by the metals will result in a current flow (I_{gal}) between the metal acting as the anode and the metal acting as the cathode in the pair. This flow can be measured without the application of an external current, which is the main advantage of this type of sensor, as this guarantees the simplicity of the sensor and measurement systems, reducing associated costs. The current flow within the macrocell can be measured using a zero resistance ammeter. According to Ohm's law, this current flow between the mentioned regions is limited by the electrolyte resistance, the anodic polarization resistance (AR) and the cathodic polarization resistance (CR) (Andrade et al., 2008; Baltazar et al., 2007). Therefore, the current induced by the coupling of the anode and cathode is proportional to the dissolution of iron in the macrocell anode (Mccarter and Vennesland, 2004).

I_{gal} should not be confused with the corrosion current density (I_{corr}), which can be obtained through the Stern-Geary equation from the value of the polarization resistance (R_p) (Martínez and Andrade, 2009) or by the electrochemical impedance spectroscopy (EIS) technique, which is still a technique widely used in the laboratory (McCarter and Vennesland, 2004) due to the overlapping of arcs from simultaneous phenomena and measurement noise associated with the heterogeneity of concrete structures in service (Ribeiro et al., 2015).

Direct estimation of the actual values of R_p from the relationship between the potential variation and the induced change in current ($\Delta E/\Delta I$) is generally not feasible in large concrete structures. This is because the applied electrical signal tends to disappear as the distance increases between the counter-electrode (CE), needed to register the parameter, and the working electrode (WE). To get around this problem, it is possible to use confinement rings in a certain area of the WE surface (Feliú et al., 1990). However, it is unfeasible to make a sensor to be embedded in concrete that, in addition to allowing the reading of the R_p, confines a specific area of the reinforcement (Martínez and Andrade, 2009).

A sensor to be embedded in concrete in order to measure R_p and I_{corr} must include in its composition a reference electrode (REF), a counter electrode (CE), and a working electrode (WE) is also required to avoid the effect of distance critical (L_{crit}) between the CE and the main reinforcement in the case that it is in a passive state. In addition to the electrochemical corrosion parameters, a thermocouple should be considered to measure temperature, as well as resistivity meters to consider the effect of varying temperature and moisture content in concrete. Therefore, the costs associated with materials and systems would increase.

The galvanic sensor is one of the most commercialized corrosion sensors on the international market. Even so, a sensor can cost around US$400, which makes it more expensive and difficult to use in public works, in addition to the limited number of suppliers (Araújo et al., 2013).

In this context, the aim of this work was to evaluate the functioning of a galvanic sensor with multiple electrodes, made with low-cost Brazilian materials. For this, the developed sensors were embedded in reinforced concrete prisms that were exposed to an aqueous solution with the addition of NaCl (3.5% by mass) in alternating cycles of partial immersion and drying. An attempt was made to simulate the service conditions of a tidal variation zone within a marine atmosphere. The work also aims to evaluate how the sensor arrangement, the concrete strength class and the effect of wetting and drying cycles can affect the readings performed.

The manufactured galvanic sensor is based on the CorroWatch Multisensor, but instead of using activated titanium as a cathode, which is ten times more expensive than conventional steel (ISE, 2020), copper was chosen. Thus, the work deals with an investigation related to the solution of problems related to quality control, damaged concrete and construction recovery, an approach that

is a recurrent theme in the Alconpat journal (Real et al., 2015; Hernández et al., 2016; Macioski et al., 2016; Pérez et al., 2018).

2. MATERIALS AND METHODS

2.1 Concrete specimens

The experimental program consisted of the analysis of the behavior of galvanic sensors installed in prismatic reinforced concrete specimens, with dimensions: (150 x 150 x 100) mm and two CA-50 steel bars with a diameter of 6.3 mm (1/4") placed parallel to each other. Figure 1 illustrates the specimen configuration. For each concrete, 4 specimens were produced, totaling 8 samples.

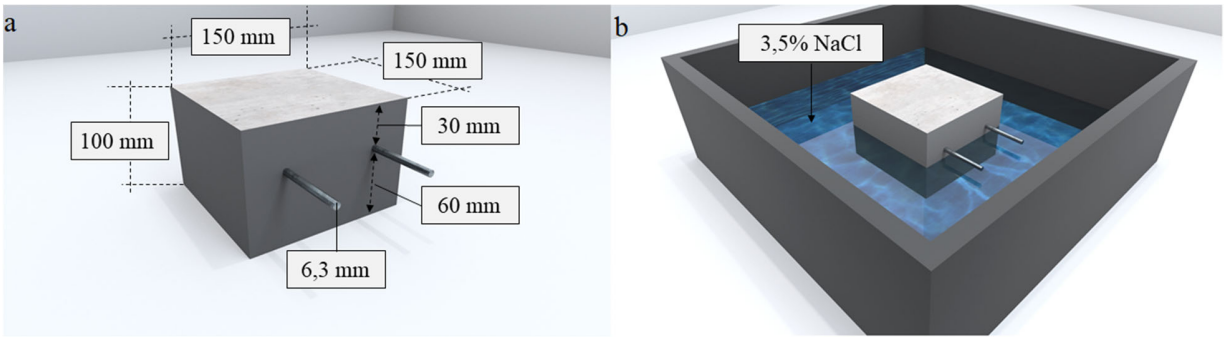

Figure 1. (a) Configuration of the reinforced prismatic concrete specimen. (b) Partially immersed specimen.

In the specimens, the cover of the main bars was defined using NBR 6118:2015 as reference, considering that the structures or some of their elements may be exposed to very strong environmental conditions (Class IV). For Class IV, the standard indicates a minimum cover (c_{min}) of 50 mm, assuming that the specimens are representative of a beam or column. In this context, the cover of the main reinforcement in relation to the surface of the specimen, exposed to the NaCl solution, was 60 mm. On the sides of the specimens and on the surface exposed to air, the bars have a 30 mm cover, as shown in Figure 1(a).

In this experiment, two concretes conventionally used in concrete plants in the region of Curitiba (Brazil) were used, as shown in Table 1. The compressive strength test in concrete (Ø10 x 20 cm cylinders) was carried out in accordance with NBR 5739 (2018). The average strength for this test was obtained from three samples for each series. The average compressive strength (f_{cm}) of concrete with (w/c) 0.75 was 20.62 MPa, and the f_{cm} of the concrete with (w/c) 0.45 was 39.36 MPa. The test was carried out with the specimens in saturated condition with a dry surface.

Table 1. Mixing ratios used for molding the specimens.

Concrete	Cement [kg/m^3]	Sand [kg/m^3]	Gravel [kg/m^3]	w/c [kg/kg]
15 MPa	242.11	970.86	997.50	0.75
30 MPa	410.04	758.58	1053.82	0.45

The 15 MPa mix simulates structural concrete from old buildings. It should be noted that structures built a few decades ago allowed characteristic strengths (f_{ck}) below 20 MPa. Furthermore, standards such as ACI 318-14 recommend a minimum f_{ck} of 17 MPa for reinforced concrete structures exposed to moisture and an external source of chlorides (Class C2). The Brazilian standard NBR 6118:1980 only established that the concrete should present a f_{ck} characteristic strength greater than 9 MPa, compatible with that adopted in the project, as well as meet the quality control criteria

provided for in ABNT NBR 12655. However, the standard NBR 6118:1980 did not include durability criteria for the execution of structural concrete according to the level of aggressiveness of the environment to which the concrete would be exposed.
The 30 MPa mix corresponds to Class III (marine or industrial atmosphere) according to NBR 12655:2006 and the updated version of NBR 6118:2014, similar to the concrete recommended by ACI 318-14 (f_{ck} = 30 MPa – w/c = 0.40) for the same exposure conditions. For the execution of the reinforced concrete specimens, the cement used was blended cement CP-II-F-32, which has up to 25% carbonaceous material (NBR 16697:2018). The fine aggregate was a fine sand, and gravel was used as the coarse aggregate. The physical characterization of the aggregates and the standards considered for this are presented in Table 2.

Table 2. Physical characterization of aggregates.

Aggregate	**Maximum characteristic dimension**	**Fineness module**	**Powder content**	**Specific mass**
Coarse (Gravel)	19.00 mm	1.83	0.39%	2.66 g/cm^3
Fine (Fine sand)	0.600 mm	2.40	9.06%	2.50 g/cm^3
Standard	ABNT NM 248:2003			ABNT NBR NM 52:2003 ABNT NBR NM 53:2003

The consistency of the concrete was measured using the slump test method, as recommended by the Brazilian standard NBR 7223: 1992. For both concretes, a fluidity in the range of 80 ± 10 mm was adopted in order to maintain a plastic consistency for molding all specimens, which did not require the use of chemical admixtures. After molding, the specimens were subjected to a curing process by immersion in water saturated with lime as indicated in the NBR 5738:2003 standard for a period of 91 days.
A cure period longer than that recommended by the standard NBR 5738:2003 (28 days) was chosen to simulate the concrete of a real structure that will have the need for field tests after a certain number of years of service. Therefore, no electrochemical readings were taken during the hardening of the concrete or during the concrete curing period. Since the objective is to simulate the interior of a real structure to evaluate the performance of the sensor, a period of stabilization of the concrete outside the curing chamber was not considered. Similar considerations were made in the work by Rocha (2012) and by Dotto (2006).
Finally, after the 91-day curing process, the specimens were placed in an oven to dry at 50°C for 5 days. Then, the lateral surfaces of the specimens were isolated from exposure to chlorides with an epoxy paint with the intention of making the contamination front only advance along the face with the 60 mm cover. To induce corrosion of the steel embedded in the concrete, an accelerated aging process that involves the absorption and diffusion of chloride ions in the cement matrix was used. Accelerated aging followed a partial immersion system alternated in cycles. The cycles consisted of drying in an oven at 50°C for 5 days and partial immersion of the specimens in water with 3.5% NaCl by mass for 2 days, as shown in Figure 1(b). This approach was adopted based on other works that used the same alternating immersion system (Freire, 2005; Dotto, 2006; Silva, 2010; Rocha, 2012; Silva, 2017).

In addition, the adopted system and the salt concentration try to reproduce service conditions similar to a tidal variation zone within a marine atmosphere. In this region, there is contact with water contaminated with chlorides, with wetting and drying cycles. This characterizes a critical exposure condition in terms of reinforcement corrosion. The main degradation mechanism present in these conditions is the corrosion of the reinforcement by the action of chloride ions (Lima and Morelli, 2004), which is the attack considered to evaluate the performance of the sensors in this research.

2.2 Sensor configuration

The galvanic macrocell considered in the study is formed by copper and carbon steel. Carbon steel bars 60 mm in length and 6.3 mm (1/4") in diameter (anode) were used at different heights and installed on a copper plate (cathode) 50 by 50 mm and 4 mm thick. All metals were polished with steel brush. Then, they were rinsed with distilled water, immersed in alcohol and air dried. The area of the copper plate that acts as the cathode (Ac) in the galvanic sensor designed in the work was configured so that it was equal to the sum of the surface area of the anodes (Aa) that make up the galvanic macrocell for an Ac/Aa ratio = 0.97. Figure 2 shows a drawing of the galvanic sensor used in the study.

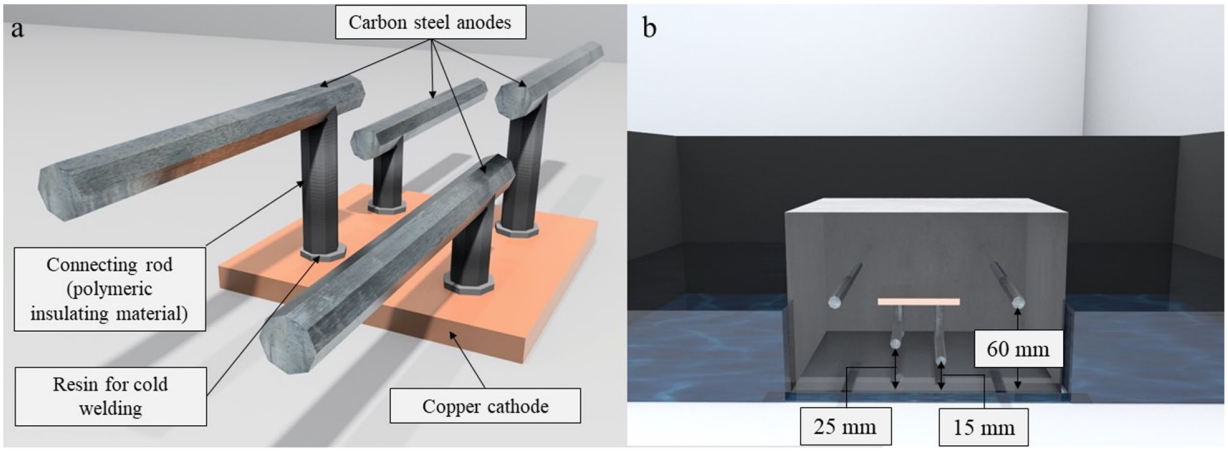

Figure 2. a) Galvanic sensor used in the study. b) Galvanic sensor installed inside the specimen. Source: Author.

Two of the sensor anodes were at a depth of 15 mm and the remaining two at a depth of 25 mm, with respect to the surface of the specimen exposed to the NaCl solution. These are the depths at which the sensor must produce the reinforcement depassivation information by the ingress of chlorides, as shown in Figure 2(b). Figure 3 shows the molding of the prismatic specimens and sensor installation.

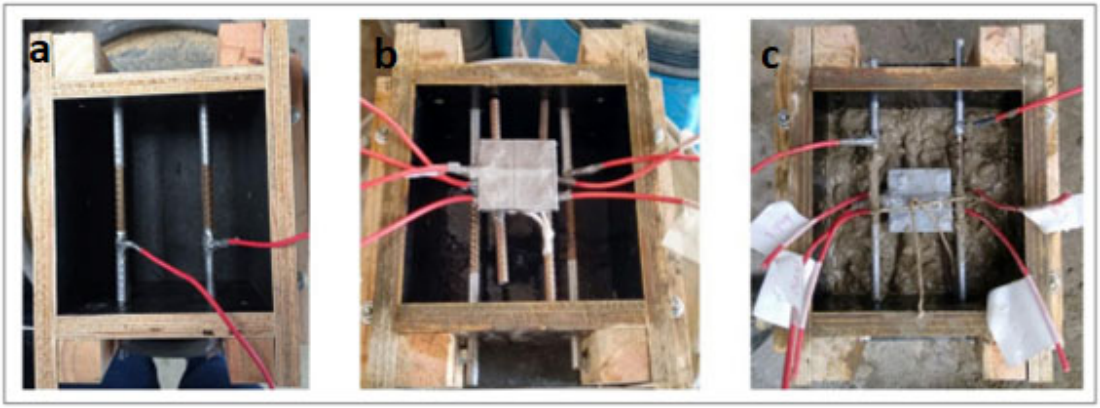

Figure 3. a) Installation of main bars. b) Molds coated with oil and with the sensor positioned. c) Molding with the sensor embedded. Source: Author.

To fit the carbon steel bars to the copper plate, 4 holes 8.0 mm in diameter (> 6.3 mm) were made, as shown in Figure 4. The carbon steel bars were fixed to the copper plate with resin for cold welding in order to avoid an unwanted galvanic couple that could compromise the proper functioning of the sensor, in addition to exposing the device to premature degradation. For the external electrical circuit that connects the electrodes and allows the flow of electrons, a copper cable insulated with a PVC film and a 2.5 mm^2 cross section was used, which was welded to the metals involved. The welding points were protected with insulating polymeric material.

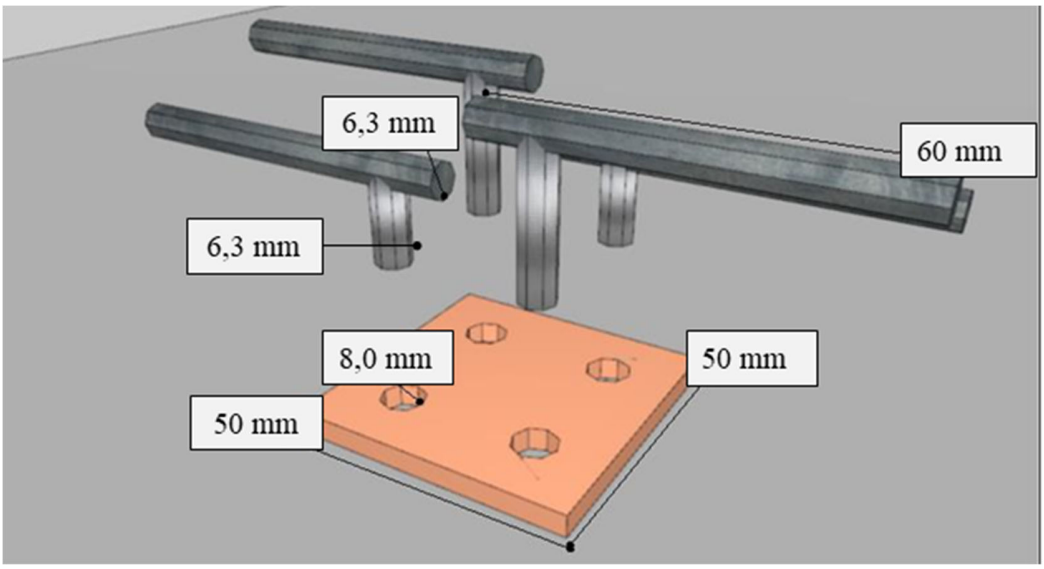

Figure 4. Sensor assembly diagram.

The choice of metals (electrodes) for the construction of the galvanic sensor was a function of the predetermined irreversible equilibrium potential (E_{eq}). Irreversible equilibrium potentials are electrode potentials that have changed under the influence of polarization or external factors. They are experimentally determined and are commonly called corrosion potentials (Gentil, 1996). To determine them, a reference electrode is used, such as a standard hydrogen electrode. E_{eq} indicates the tendency of the electrode to undergo reduction or oxidation in a given medium. The greater the corrosion potential of the electrode in a table of potentials, the greater the tendency of the electrode to undergo oxidation, that is, to behave like an anode (Gentil, 1996; Pawlick et al., 1998; Souza, 2014).

The irreversible equilibrium potential of iron immersed in an electrolyte simulating sea water with reference to a hydrogen electrode is in the range of (-0.34 to 0.50) V. However, the corrosion potential of copper is in the range of (-0.02 to 0.05) V (Akimov, 1957). In the study, the corresponding experimental procedure was not carried out to determine the irreversible potential value of the cathode and anode separately.
Finally, in order to make the sensor more practical, protect the copper cables and consequently improve the recording of electrochemical readings, electrical pin connectors were placed at all ends, as shown in Figure 5(b).

2.3 Characterization tests and electrochemical techniques

At each exposure cycle, electrochemical readings were conducted on the second day of partial immersion in water with 3.5% NaCl. In order to determine the potential of the sensor pairs throughout the aging process, the LabVIEW 8.5 data logger was used, which recorded the polarization potential difference (E_{pair}), as shown in Figure 5.

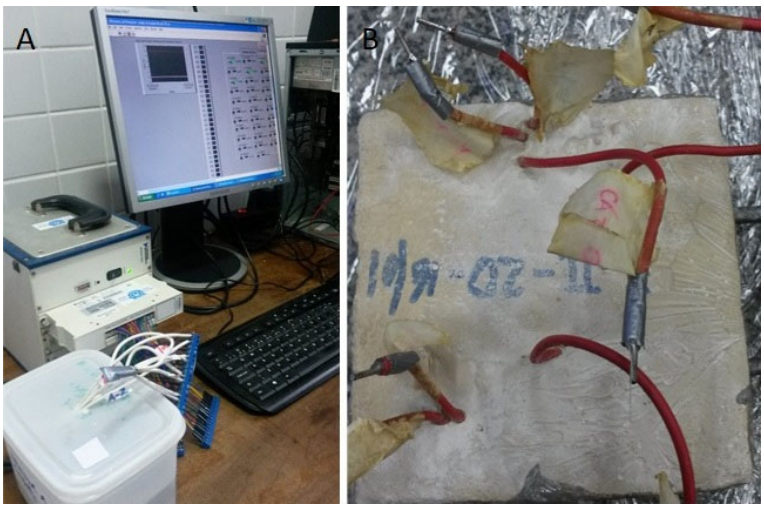

Figure 5. a) LabVIEW 8.5 data logger reading E_{pair}. b) Specemin with electrical pin connectors. Source: Calvo, (2018).

Theoretically, the potential of a galvanic couple (E_{pair}) is the result of the combination of the potentials of the metals involved. It is a spontaneous process caused by the different nature of the electrodes that leads to the polarization of both metals to a combined potential (E_{pair}) (Gentil, 1996; Pawlick et al., 1998). That is, it is obtained from the difference between the positive potential corresponding to the cathode ($E_{cathode}$) and the negative potential (E_{anode}) corresponding to the anode, as shown in Equation (1) (Pawlick et al., 1998) in the environment in which they are inserted.

$$E_{pair} = E_{cell} = E_{cathode} - E_{anode} \quad (1)$$

In practice, $E_{cathode}$ is the polarization potential of the cathode and E_{anode} is the polarization potential of the anode. The polarization potential is the result of the displacement (η) of the metal's irreversible equilibrium potential (E_{eq}) by the formation of the galvanic couple. Thus, Equation 1 can be written in the form of Equation (2).

$$E_{pair} = \left(E_{eq} + \eta\right)_{cathode} - \left(E_{eq} + \eta\right)_{anode} \quad (2)$$

As no external current is applied to the galvanic macrocell, the polarization potential of the electrodes (anode and cathode) is always in the range of the natural potential of the metals inside the concrete (Mccarter and Vennesland, 2004). Therefore, the E_{pair} value will fluctuate as a function of environmental conditions (Pawlick et al., 1998). Thus, the E_{pair} value must be obtained empirically (Sousa, 2014), and its value includes the values of E_{pair} and η, dispensing with the determination of these factors separately.

Thus, the data logger generated an individual reading corresponding to each of the anode-cathode pairs of the projected sensor. Each pair is recognized by the logger as an individual reading channel. It was analyzed whether the potential difference reading remains stable over time, as well as the type of reaction it indicated: galvanic ($E_{pair} > 0$) or electrolytic ($E_{pair} < 0$).

To record the galvanic current (I_{gal}), the electrochemical technique was used, using a Zero Resistance Ammeter – ZRA coupled to an SP-200 potentiostat and logging via EC-Lab software. This technique consists of measuring the galvanic current in a pair formed by different metals, one with an anodic behavior and the other with a cathodic behavior.

The technique is also used to perform some types of electrochemical noise measurements and consists of stabilizing the voltage between the working electrode and the counter electrode, and measuring the current and potential versus the reference electrode (EC-LAB., 2011). In this case, the working electrodes are the carbon steel bars of the galvanic sensor. As a counter-electrode, a stainless steel mesh was used and the reference electrode was the copper plate of the sensor.

In order to help validate the behavior of the sensor, the galvanic current and potential readings of the pair were correlated with the open circuit potential (E_{corr}) readings. Due to its simplicity, measuring the corrosion potential, E_{corr}, is the most used method in field determinations (Martínez and Andrade, 2009). From these measurements, potential maps are drawn revealing the zones that are most likely to corrode in the active state (ASTM C876-15).

A reading was taken at each anode, totaling 6 readings per specimen: four on the sensor anodes and two on the reinforcement bars. In the potential difference readings, a $Cu/CuSO_4$ reference electrode was used. To analyze the results in order to estimate the probability of corrosion in a given structure, the limits found in ASTM C876-15 were considered.

However, there is still no regulation that establishes a fixed range of I_{gal} and E_{pair} values to characterize the active state of steel in concrete. Therefore, it is not the absolute value of the current that should be considered, but the variation of its values over time (Raupach and Schiessl, 2001; Araújo et al., 2013).

Finally, a qualitative test was performed using the colorimetric method by spraying silver nitrate ($AgNO_3$) to determine the depth of the penetration front of chlorides entering the concrete by absorption and diffusion, although it does not quantify the free chloride content (Real et al. al., 2015; France, 2011, Pontes et al., 2020). The test consists of spraying an aqueous solution of 0.1 M $AgNO_3$ onto freshly fractured concrete slices. When the silver nitrate solution is sprayed onto the concrete surface, a photochemical reaction takes place. A white precipitate of silver chloride forms where free chlorides are present. In the region without chlorides or with combined chlorides, there is formation of a brown precipitate, silver oxide (Medeiros, 2008; Marcondes, 2012).

To carry out the test, the specimens were broken in the direction of the flow of chlorides just before the test to prevent carbonation from occurring. In parallel, a test with phenolphthalein spray (1% in ethyl alcohol) was also performed on one of the specimens' slices to avoid false positives. In the presence of carbonates there is also the formation of a white precipitate (Jucá, 2002).

After spraying the aqueous solution of silver nitrate, ten measurements of the depth of penetration of chlorides were performed, every 10 mm, following the recommendations of NT BUILD 492 (2000). In this way, gross errors were avoided in reading the depth reached by chlorides. Before spraying the silver nitrate and phenolphthalein, each slice was brushed to remove surface dust.

3. RESULTS AND DISCUSSION

3.1 Corrosion Potential

Figure 6 shows the results of Open Circuit Potential (E_{corr}) in specimens with 15 MPa concrete. Figure 7 shows the data corresponding to specimens with 30 MPa concrete. Both figures show the average of the readings obtained from the anodes of the galvanic sensor installed inside the specimens, with a cover thickness of 1.5 cm and 2.5 cm, respectively. Also represented in these figures are the averages corresponding to the main bars with a cover thickness of 6 cm.

At the end of the first wetting cycle, negative Ecorr values (< -350 mV) were observed in the anodes installed at 1.5 cm and 2.5 cm, in both concretes. Several studies found more negative values (indicating active corrosion) at the start of corrosion tests (Gurdián et al., 2014; Rocha et al., 2014; Capraro et al., 2016; Jiang et al., 2017; Medeiros et al., 2014; , 2017; Godinho et al., 2018; Godinho et al., 2019; and Capraro et al., 2021). This behavior is related to the process of formation of the passivating film on the reinforcement, which involves the oxidation of the metal surface and, for this reason, generates electronegative readings at the beginning of the test (Poursaee, 2016; Meira, 2017; Ribeiro et al., 2018).

Thus, E_{corr} gradually changes, transitioning from more negative values to more positive values, until it stabilizes and indicates the formation of the passivating film (Sun et al., 2017) in the absence of aggressive agents inside the concrete. Capraro et al. (2021), for example, observed high negative values (-600 mV / -700 mV) from the start of monitoring up to 800 days in all series exposed to dry chamber wetting and drying cycles (55 ± 5% R.H. and 23 ± 2 °C). Similarly, Godinho et al. (2018) observed readings in the range of -486 mV to -550 mV up to 100 days.

In order to encourage the formation of passive film on steel bars before molding, Ghods et al. (2010), Nahali et al. (2014), Williamson and Isgor, (2016) and Godinho et al. (2019) suggest the immersion of carbon steel bars in synthetic solutions that simulate the interior of the concrete before molding.

In this work, the monitoring of anodes installed at 1.5 cm and 2.5 cm did not show a stabilization level, but a tendency to become more electronegative as the chloride content inside the concrete increased.

With regard to the durability of concrete, ABNT NBR 6118 (2014) stipulates minimum cover values (c_{min}) on the reinforcement according to the aggressiveness of the environment in which the structure is inserted. In this case, for the galvanic sensor anodes (1.5 and 2.5 cm), these values were intentionally not respected. Adding to this the interconnectivity between the existing pores and micro-cracks in the paste, the efficiency of the physical protection that the cover provides is reduced.

According to Leek (1991) and Ribeiro et al. (2014), even with the alkaline reserve product of the $Ca(OH)_2$ content in concrete and the passivation film, the presence of chlorides inside the concrete can trigger the dissolution of the passive film and initiate the corrosive process. According to the authors Huafu et al. (2015) and Jin et al. (2017), as the degree of contamination by chlorides increases, the more negative the E_{corr} value tends to become.

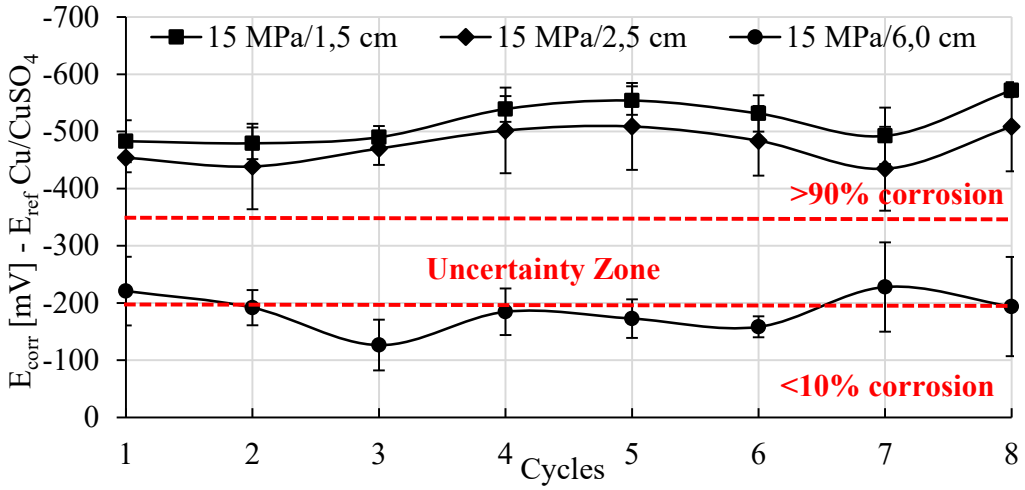

Figure 6. Corrosion potential for the 15 MPa mix. Source: Author.

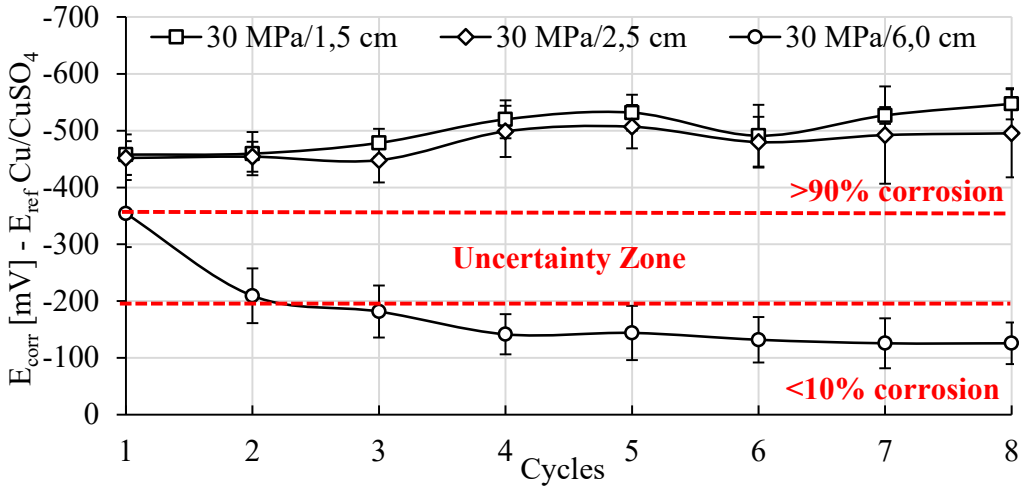

Figure 7. Corrosion potential for the 30 MPa mix. Source: Author.

On the other hand, in the main bars with 6 cm of cover, the probability of corrosion was less than 10% or in the range of (-200 to -350 mV) for both concretes. A similar behavior was observed by the authors Romano et al. (2013), who studied the performance of a sensor with electrodes at different depths in relation to the exposed surface of the specimen, namely: 1.5 and 3 cm. In the study, the electrode placed at a lower depth indicated depassivation before the electrode with a 3 cm cover. In addition, reinforcement bars of the specemin with a 4 cm cover depassivated 100 days after the sensor electrode was placed at a shallower depth.

Theoretically, more electronegative E_{corr} values indicate a critical level of chloride ions around the sensor anodes. If anodes are installed at different depths, anodes closer to the outer surface, through which ion penetration takes place, should present more electronegative values faster than those anodes located at greater depth (Romano et al., 2013).

Finally, the ANOVA analysis of variance and the subsequent Tukey test with 95% confidence indicated that the concrete strength did not influence the results obtained during the corrosion potential test. Therefore, the behavior of this quantity in the specimens of both mixes was the same.

3.2 Pair potential

Figures 8 and 9 show the average potential values of the pair for the six anodes of the system (corrosion sensor + steel bar). For 15MPa concrete, when the potential value of the pair was

negative, the probability of anode corrosion was less than 10% or was in the uncertainty zone according to the open circuit potential readings.

Based on the results observed in this work, 20 mV/min is the potential value of the pair (E_{pair}) for the arrangement and metals used (carbon-copper steel), which characterizes the tested galvanic couple. In parallel, the threshold of 200 mV/min appears to indicate the change to the active state (indicated with a dashed line in Figures 8 and 9).

Thus, when the potential of the pair is in the range of 20 to 200 mV/min, as in the case of anodes with 1.5 cm and 2.5 cm cover in the first cycles, the corrosion is in the active state. From the 4th cycle onwards, the potential of the pair was greater than 200 mV/min, and the anodes were definitely in the active state, regardless of the cover. Positive E_{pair} values indicate that the oxidation process predominates over the reduction process and the anode corrodes (anodic polarization). The greater the potential difference in the galvanic couple, the more intense the anodic polarization tends to be (Pawlick et al., 1998, Sousa, 2014; Fernandes and Martendal, 2015) and the more intense is the corrosion reaction in the pair.

For the 30MPa concrete (Figure 9), a similar behavior was observed for the six anodes at 1.5, 2.5 and 6.0 cm depth. The concrete strength did not influence the results obtained during the pair potential test, according to statistical analysis (ANOVA and Tukey at 95% confidence). It is also noteworthy that the average error of the E_{pair} readings is small when compared to E_{corr} (Figs 6 and 7). Thus, it is possible to prove greater stability in the readings taken with the galvanic sensor.

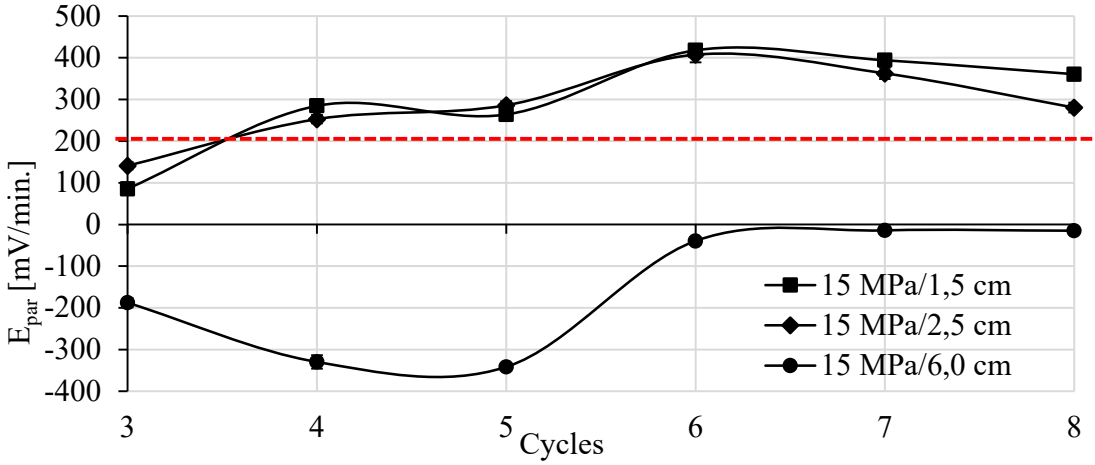

Figure 8. Pair potential for the 15 MPa mix. Source: Author.

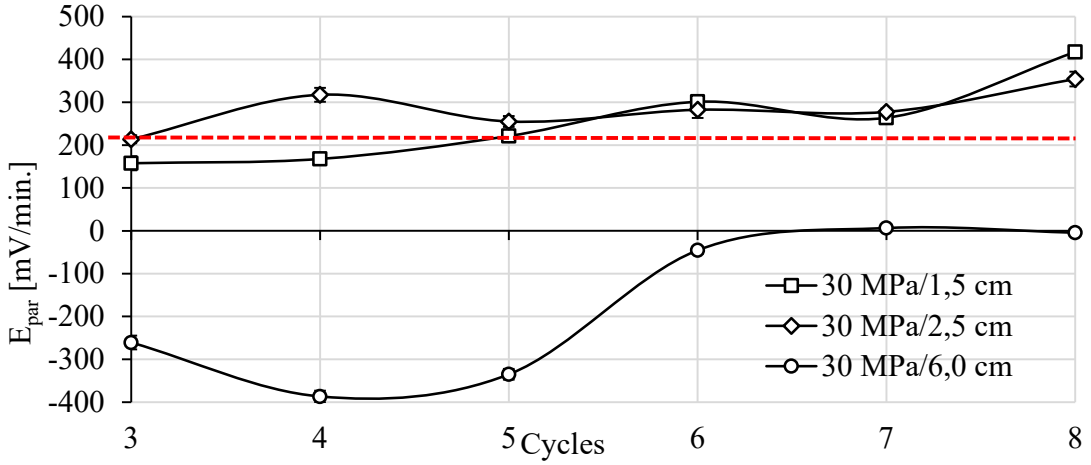

Figure 9. Pair potential for the 30 MPa mix. Source: Author.

Angst and Buchler (2015) expose some intrinsic difficulties in monitoring the mixed potential of a galvanic macrocell (E_{pair}): (i) anodic and cathodic reactions generally occur in the same structural element, (ii) or it is not possible to place reference electrodes near the anode and cathode (iii) or the electrolyte conductivity is too high and therefore the potential difference is too low to be accurately measured.

Note, however, that Angst and Buchler (2015) refer to a macrocell formed on the surface of a steel bar, a product of the penetration of chlorides into the concrete that causes localized corrosion. A galvanic sensor, in a different way, is formed by small pieces of metal with different electrical potentials where one will act as an anode and the other as a cathode, embedded in the concrete at depths always smaller than that of the reinforcement (Andrade et al., 2008; Araújo et al., 2013), which reduces the influence of the conductivity of the electrolyte.

It then remains to consider aspect (ii) mentioned by the authors: the possibility of placing reference electrodes close to the anode and cathode. Thus, in future tests that use the galvanic sensor proposed in this research, it is recommended to install a reference electrode as well. This practice will make it possible to separately determine the anode and cathode potential and thus be able to determine the polarization curve of each electrode, improving the monitoring of the galvanic couple potential.

It is also suggested to monitor the behavior of the potential of the pair (E_{pair}) in an environment free of aggressive agents until the parameter reaches an equilibrium point in the range of positive values, as its value is a function of the potentials of the metals that make up the galvanic couple inside the concrete (Pawlick et al., 1998; Mccarter and Vennesland, 2004).

However, the stability of the sensor potential over time is also influenced by the anodic and cathodic current densities. In turn, the anodic and cathodic currents are a function of the anode area and the cathode area, respectively (Pawlick et al., 1998).

Therefore, if the anode has insufficient area, the potential of the pair will shift to higher values with an upper limit represented by the open circuit potential of the metal acting as the cathode. As the area of the cathode in relation to the anode increases, the demand for electrons from the cathode increases, while the area of the anode from which the electrons will be supplied decreases and, therefore, the rate of dissolution of the anode increases (Sousa, 2014). Under these conditions, there is a risk that the anode degrades excessively and shortens the lifetime of the sensor. Therefore, the behavior of the galvanic sensor must be evaluated with a cathode/anode area (A_C/A_A) ratio equal to 1, in order to improve the functioning of the sensor proposed in the work.

Initially, the experimental program did not foresee the realization of this test, but it proved to be extremely important to understand the behavior of the sensor over time.

3.3 Galvanic current

Theoretically, when a corrosive process is established in the bars, the galvanic current increases in the range of positive values due to the variation in the anode potential, which assumes more negative values compared to those obtained initially in its passive state (Araújo et al., 2013; Lacerda and Muller, 2015). An increase in galvanic current accompanied by a decrease in the open circuit potential indicates that a critical level of chloride ions has been reached (Andrade et al., 2008; Araújo et al., 2013).

In Figures 10 and 11 it is possible to observe that during monitoring, the galvanic current (I_{gal}) was negative during seven of the eight cycles in the six monitored anodes (four from the galvanic sensor and the two main bars). For the 15 MPa concrete (Figure 10), positive galvanic current values were observed in cycle 7 after 141 days of monitoring. However, they became negative again in cycle 8. For the 30 MPa concrete, in Figure 11 it is observed that the galvanic current was positive in cycles 7 and 8.

In principle, positive current values are in agreement with the open circuit potential more negative than -350 mV (corrosion probability > 90%), and with the pair potential greater than 200 mV/min, observed at the anodes installed at a lower depth (1.5 and 2.5 cm).

However, in the main bars installed with 6 cm of cover, E_{pair} indicated an electrolytic reaction during the monitoring, which means that the bars were in a passive state in agreement with the measured open circuit potential value. Therefore, the positive galvanic current (I_{gal}) record did not correspond with what was observed in the bars in the previous tests.

However, the galvanic current was close to zero throughout the test. Galvanic current values close to zero are also indicative of the steel's passive condition (Park et al., 2005; Sousa, 2014). Thus, similarly to what happened in the first stage of the experimental program with the sensors soaked in an aqueous solution (Calvo et al., 2017), I_{gal} showed greater inertia to identify the presence of an aggressive agent. Furthermore, according to Ribeiro and Cunha (2014), the galvanic current (I_{gal}) decays throughout the measurement, showing a capacitive behavior which makes monitoring difficult.

The results of galvanic current obtained in the six anodes (1.5, 2.5 and 6 cm) installed in the specimens of the 15 MPa mix were statistically equivalent to the values of galvanic current recorded in the anodes installed in the test specimens of the 30 MPa mix.

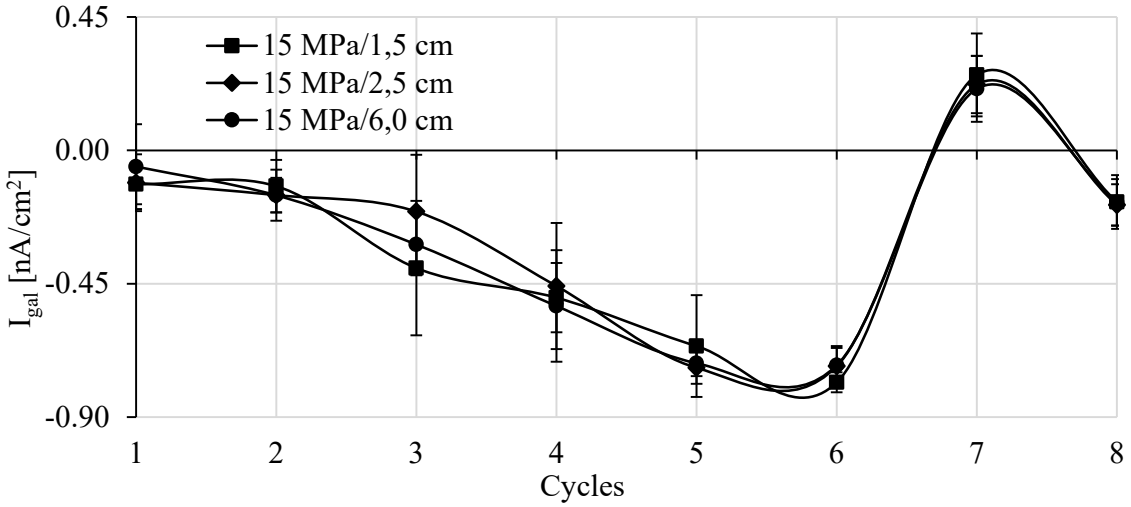

Figure 10. Galvanic current for the 15 MPa mix. Source: Author.

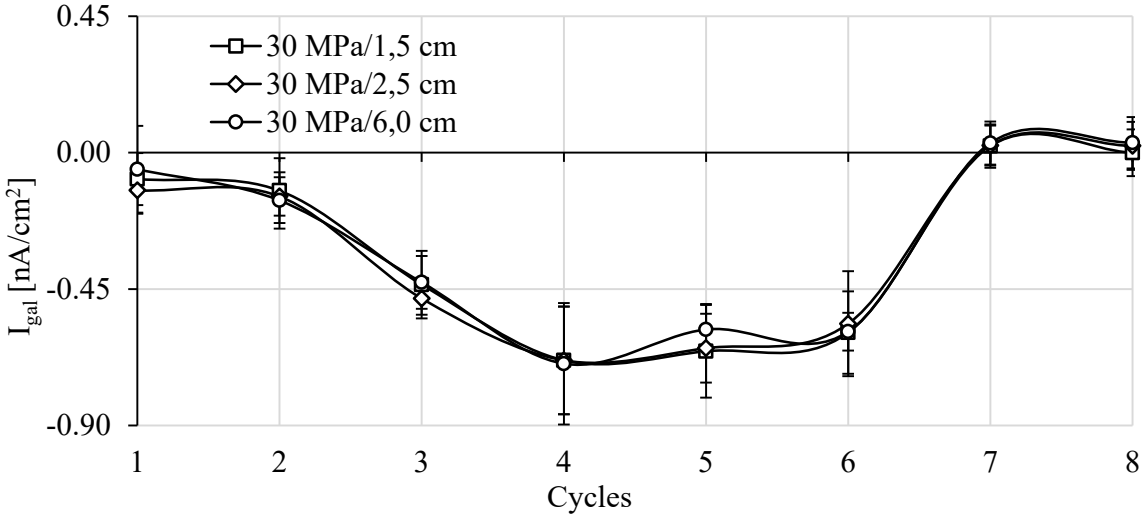

Figure 11. Galvanic current for the 30 MPa mix. Source: Author.

Finally, for data analysis, the linear model was applied, with the determination of R^2 to infer the correlation between the electrochemical techniques considered in the work. No correlation factor (R^2) came close to 0.9; therefore, it cannot be affirmed that there is a positive linear relationship between the electrochemical techniques. That is, the measured quantities differ and do not converge. For this reason, this type of study is important, as the choice of the correct technique, or set of techniques, is essential for the monitoring to be efficient. However, the suggestions made earlier in order to improve the functioning of the sensor are essential in order to be able to understand and estimate the behavior of the quantities evaluated in the field accurately.

3.4 Chloride penetration by the colorimetric method

At the end of the corrosion monitoring, colorimetric tests with silver nitrate ($AgNO_3$ 0.1 M) and phenoltalein were performed. Figure 12 shows the appearance of the specimen slices after spraying the indicators. In none of the eight specimens tested was carbonated concrete observed, as indicated by the pink color in one of the specimen slices. This evidence that there is no carbonation in concrete is important to be sure that the colorimetric test of spraying a solution with silver nitrate will be effective, without indicating the false positive alerted in the works by Pontes et al. (2020).
In the slice on the left, it is possible to see two distinct regions in terms of color: one with a brown precipitate corresponding to the region without free chlorides, and another without color in the region affected by free chlorides, which indicates how far the chloride penetration front has reached. In Figure 12, the region without chlorides was delimited with a black line.
After 150 days at the end of the eighth cycle, the chloride penetration front reached an average depth of 7.6 cm in the 15 MPa concrete specimens and 7.2 cm in the 30 MPa concrete specimens. Therefore, in the concrete around the sensor anodes, a critical level of chlorides was reached. The results obtained on the sensor anodes during the E_{corr} and E_{pair} tests indicated a high probability of corrosion at the end of the test.

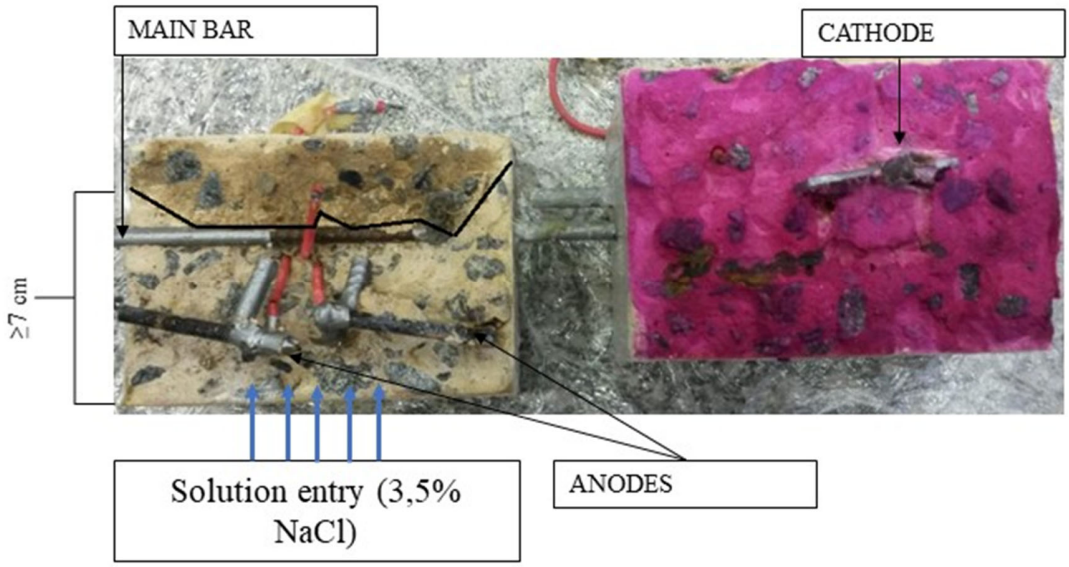

Figure 12. Colorimetric test (chloride penetration and carbonation) in the specimen after the end of monitoring.

It is observed that the depth of penetration of chlorides at the end of the cycles was similar between the 15 MPa and 30 MPa concretes. In this sense, it is necessary to point out that as well as porosity, cracking also provides facilities for aggressive agents to penetrate the concrete and initiate their destructive action in the structure. After the mass hardens, cracks are the result of drying shrinkage,

reinforcement corrosion and alternating wetting and drying cycles, among other factors (Brandão and Pinheiro, 1999). In this work, the three factors acted in combination, providing the appearance of microcracks, as shown in Figure 13.

The appearance of microcracks may have intensified the capillary penetration of water with chlorine ions, causing the concrete to present similar behaviors, different from what was observed under natural exposure conditions. Thus, drying in an oven at 50^0C does not seem adequate and should be re-evaluated in other similar studies. However, studies that evaluated the penetration of chlorides in different Brazilian cements observed that concretes with CP-II-F have a high capacity for penetration of chlorine ions when compared to other types of cement, thus reducing the influence of the w/c ratio (Pereira, 2001; Crauss, 2010; Fleet et al., 2018).

Figure 13. Microcracks in specimens.

On the other hand, even though the chloride penetration front reached the main bars (6 cm cover), the critical chloride content for the depassivation of the reinforcement was not reached in the concrete at this depth. This is because the probability of corrosion was less than 10% or in the uncertainty zone, whereas E_{pair} indicated an electrolytic reaction, or at most was in the range -5 to 20 mV/min.

In this sense, it is necessary to point out that the arrival of chlorides in the vicinity of the reinforcement, by itself, does not represent the beginning of the corrosion process. The process will only start when the Cl- ion content around the steel bar reaches the critical content (Jin et al., 2017) in order to depassivate the steel.

Most standards set the permitted Cl- ion contents in relation to the cement mass. Although it is a very controversial point, the value of 0.4% in relation to the cement mass is a consensus in most standards (Cascudo, 1997). The NP EN 206 standard, for example, adopts the value of 0.4% (Silva, 2017) and ABNT NBR 12655 (2006) establishes 0.15% in the structure's service conditions.

Furthermore, by breaking the specimens, it was possible to confirm the presence of the corrosion product around the sensor bars, but not around the exposed part of the main bars (6 cm cover). It should be noted that the ends of the main bars were protected with gray insulating tape, so that only 60 mm of the bar was exposed, the same length as the sensor anodes, as shown in Figure 3(a).

4. CONCLUSIONS

The aim of this work was to evaluate the efficiency of a galvanic sensor with multiple electrodes in monitoring the corrosion of reinforced concrete prisms, comparing it with conventional electrochemical methods and with the depth of penetration of chlorides. As the main conclusions of the study, the following can be mentioned:

- The w/c ratio did not influence the tests, with cover being the factor that exerted the greatest influence.
- The open circuit potential and the pair potential indicated an active corrosion state at the sensor anodes (1.5 and 2.5 cm) rather than at the main bars (6 cm).
- For the purpose of this research, 20 mV/min is the potential value of the pair (E_{pair}), which characterizes the tested carbon-copper galvanic steel pair. The 200 mV/min threshold appears to indicate change to the active state.
- The galvanic current showed little variation over time, with capacitive behavior during the 150 days of monitoring.
- The penetration front reached a depth greater than 7 cm, reaching the main bars (6 cm). For this reason, the tests indicated a tendency for the bar to enter the uncertainty zone until sufficient concentrations of chlorides are reached to depassivate the reinforcement and initiate corrosion.
- The developed sensor showed sensitivity to detect the front of chlorides and predict the possibility of corrosion of the reinforcements. Adjustments are still needed, such as monitoring the behavior of the pair potential (E_{pair}) and the corrosion potential (E_{corr}) in a medium free from aggressive agents until the E_{pair} stabilizes. It is considered that the parameters E_{corr}, E_{pair} and I_{gal} behave differently as corrosion monitoring parameters.

5. ACKNOWLEDGMENTS

The authors thank the Laboratory of Materials and Structures of the Federal University of Paraná (LAME-DCC-UFPR), the Graduate Program in Civil Engineering (PPGEC-UFPR), the Center for Studies in Civil Engineering (CESEC-UFPR), the Coordination for the Improvement of Higher Education Personnel (CAPES), the National Water Agency (ANA) and the National Council for Scientific and Technological Development (CNPq).

6. REFERENCES

American concrete institute (ACI) (2014). ACI 318-14: *Building Code Requirements for Structural Concrete*.

Associação Brasileira de Normas Técnicas (ABNT) (1980). NBR 6118: *Projeto e execução de obras de concreto armado.*

Associação Brasileira de Normas Técnicas (ABNT) (2006). NBR 12655: *Concreto de cimento Portland – Preparo, controle e recebimento – Procedimento.*

Associação Brasileira de Normas Técnicas (ABNT) (2014). NBR 6118: *Projeto de estruturas de concreto – Procedimento.*

Associação Brasileira de Normas Técnicas (ABNT) (2003). NM 248: *Agregados - Determinação da composição granulométrica.*

Associação Brasileira de Normas Técnicas (ABNT) (2009). NBR 7211: *Agregados para concreto – Especificação.*

Associação Brasileira de Normas Técnicas (ABNT) (2003). NM 52: *Agregado miúdo - Determinação da massa específica e massa específica aparente.*
Associação Brasileira de Normas Técnicas (ABNT) (2003). NM 53: *Agregado graúdo – Determinação de massa específica, massa específica aparente e absorção de água.*
Associação Brasileira de Normas Técnicas (ABNT) (1992). NBR 7223: *Concreto - Determinação da consistência pelo abatimento do tronco de cone.*
Associação Brasileira de Normas Técnicas (ABNT) (2003). NBR 5738: *Concreto — Procedimento para moldagem e cura de corpos de prova.*
Associação Brasileira de Normas Técnicas (ABNT) (2018). NBR 5739: *Concreto — Concreto - Ensaio de compressão de corpos de prova cilíndricos.*
Associação Brasileira de Normas Técnicas (ABNT) (2018). NBR 16697: *Cimento Portland - Requisitos.*
ASTM Internacional. (2015). ASTM C876 – 15 *Standard Test Method for Corrosion Potentials of Uncoated Reinforcing Steel in Concrete.* Edição atual aprovada em 1 de novembro de 2015. Publicado em abril de 2016. Originalmente aprovado em 1977. Última edição anterior aprovada em 2009 como C876-09. doi: https://doi.org/10.1520/C0876-15
NT BUILD 492 (2000), *Non-Steady State Chloride Migration (Diffusion Coefficient).*
Araújo, A., Panossian, Z., Portella, P. D., Bässler, R. (2013), Monitoramento da corrosão em estruturas de concreto: sensor galvânico. *Revista Téchne*. Edição 194. Maio/2013. Link: http://techne.pini.com.br/engenharia-civil/194/artigo294083-1.aspx
Andrade, C., Figueiras, H., Félix, C., Coutinho, J. S. (2008), *"Desempenho do kit-sensor de corrosão na monitorização da durabilidade de estruturas de betão"*, in: Anais do Encontro Nacional Betão Estruturas - BE2008. Guimarães. 5, 6, 7 de novembro de 2008.
Angst, U., Buchler, M. (2015), On the applicability of the Stern–Geary relationship to determine instantaneous corrosion rates in macro-cell corrosion. *Materials and Corrosion*. 66(10). doi: https://doi.org/10.1002/maco.201407997
Akimov, G. V. (1957), "*Théorie et Méthodes d´ Essais de la Corrosion des Métaux*". Dunod. Paris. p 53.
Baltazar, M., Almeraya, F., Nieves, D., Borunda, A., Maldonado, E., Ortiz, A. (2007). *Corrosión del acero inoxidable 304 como refuerzo en concreto expuesto a cloruros y sulfatos.* Scientia Et Technica, XIII (36),353-357. Acesso em: 17 de Julio de 2021. ISSN: 0122-1701. Disponible en: https://www.redalyc.org/articulo.oa?id=84903663
Brandão, A. M. S.; Pinheiro, L. M. (1999), *Qualidade e durabilidade das estruturas de concreto armado: aspectos relativos ao projeto.* Cadernos de Engenharia de Estruturas. n.8. EESC. Universidade de São Paulo. São Carlos. 1999.
BioLogic Science Instruments (2011), EC-LAB Software: Techniques and Applications. Version 10.1x. Fevereiro, Disponível em: https://www.egr.msu.edu/~scb-group-web/blog/wp-content/uploads/2012/07/EC-Lab-software-Techniques-and-Applications-manual.pdf
Cheng, Y., Asad H., Chen, E., Ma, G., Li, Z. (2018), *Simulation of a novel capacitive sensor for rebar corrosion detection.* Construction and Building Materials. 174: 613–624. https://doi.org/10.1016/j.conbuildmat.2018.04.133
Chen, Y., Tang, F., Tang, Y., O'Keefe, M. J., Chena, G. (2017), *Mechanism and sensitivity of Fe-C coated long period fiber grating sensors for steel corrosion monitoring of RC structures.* Corrosion Science. 127: 70–81. https://doi.org/10.1016/j.corsci.2017.08.021
Calvo Valdés, A., Farias Medeiros, M. H., de Jesus Roque, P. (2017). *Sensores de corrosão para monitoramento de pontes e viadutos de concreto armado. Primeira etapa – Testes em solução aquosa.* Revista De Engenharia E Pesquisa Aplicada, 2(3). https://doi.org/10.25286/repa.v2i3.689

Calvo Valdés, A. (2018), *"Sensores de corrosão para monitoramento de pontes e viadutos de concreto armado"*. Dissertação (Mestrado). Programa de Pós-graduação de Engenharia de Construção Civil – PPGECC. Universidade Federal do Paraná, Setor de Tecnologia, Curitiba.
Cascudo, O. (1997), *"O controle da corrosão de armaduras em concreto. Inspeção e técnicas eletroquímicas"*. Capítulo 2: Corrosão de armaduras em concreto. p 39-61. Capítulo 8: Potenciais de corrosão p 137-153. Primeira versão 1997.
Capraro, A. P. B., Gervasio, S., Medeiros, M. H. F., Hoppe Filho, J., Braganca, M., Oliveira, I. (2016), *"Avaliação dos mecanismos de corrosão de concretos contaminados com diferentes teores de pirita (FeS2)"*, in: Anais do 58o Congresso Brasileiro de Concreto (58o CBC 2016). Instituto Brasileiro do Concreto – IBRACON. Belo Horizonte/MG, 1–16.
Capraro, A. P. B., Macioski, G., Medeiros, M. H. F. (2021), *Effect of aggregate contamination with pyrite on reinforcement corrosion in concrete.* Engineering Failure Analysis. 120: 1350-6307. https://doi.org/10.1016/j.engfailanal.2020.105116
Crauss, C. (2010), *"Penetração de cloretos em concretos com diferentes tipos de cimento submetidos a tratamento superficial"*. Dissertação de mestrado. Programa de Pós-Graduação em Engenharia Civil Universidade Federal de Santa Maria. 31 de agosto de 2010.
De Lacerda, M. M., Müller, R. (2015), *Uso de sensor de taxa de corrosão instantânea como técnica de monitoramento da corrosão em estruturas de concreto*. Obra24horas. Acesso em: novembro / 2015. Disponível em: https://www.obra24horas.com.br/artigos/concreto/uso-do-sensor-de-taxa-de-corrosao-instatanea-como-tecnica-de-monitoramento-da-corrosao-em-estruturas-de-concreto
De Lima, Ma. G., Morelli, F. (2004), "*Caracterização da agressividade do ambiente marinho às estruturas de concreto*". Curso de Pós-Graduação em Engenharia de Infraestrutura Aeronáutica - ITA, São José dos Campos, SP. p 1-20 2004. Disponível em: https://semengo.furg.br/images/2004/07_2004.pdf
Dotto, J. M. R (2006*), "Corrosão do aço induzida por íons cloreto – uma análise crítica das técnicas eletroquímicas aplicadas ao sistema aço-concreto com ou sem pozolana"*. Dissertação (Doutorado). Escola de Engenharia. Programa de Pós-graduação em Engenharia de Minas, Metalúrgica e de Materiais – PPGEM. Universidade federal do Rio Grande do Sul. Porto Alegre.
Dong, S.-G., Lin, C.-J., Hu, R.-G., Li, L.-Q., Du, R.-G. (2011), *Effective monitoring of corrosion in reinforcing steel in concrete constructions by a multifunctional sensor.* Electrochimica Acta. 56(4): 1881–1888. https://doi.org/10.1016/j.electacta.2010.08.089
Freire, K. R. R (2005), *"Avaliação do desempenho de inibidores de corrosão em armaduras de concreto"*. Dissertação de mestrado. Programa de Pós-graduação em engenharia de construção civil – PPGECC. Universidade Federal do Paraná. Curitiba 2005.
França, Clério Bezerra (2011), *"Avaliação de cloretos livres em concretos pelo método de aspersão de solução de nitrato de prata"*. Dissertação de mestrado. Programa de pós-graduação em Engenharia de Construção Civil. Universidade Católica de Pernambuco. Pró -Reitoria Acadêmica- PRAC.
Fernandes, K. V., Martenda, P. C. (2015), *Por que os metais sofrem corrosão?* Engenheiro de Materiais. Acesso em: novembro 2015. Disponível em: http://engenheirodemateriais.com.br/tag/pilha-galvanica/
Figueiredo, E. J P., Meira, G. R. (2013), *Boletim Técnico: Corrosão das armaduras de concreto*. Boletín No. 6, Associação Latinoamericana de Controle da qualidade, Patologia e Recuperação da Construção. ALCONPAT Internacional.
Federal Highway Administration (FHA) (2011). *U.S. Government of Transportation. Bridge preservation guide.* August 2011.
Feliú, S., González, J. A., Feliú Jr., S., Andrade, M. C. (1990), *Confinement of the electrical signal or in-situ measurement of polarization resistance in reinforced concrete.* ACI Materials Journal. 87 (5):457.

Frota, W.D.S.; Martins, E. R.; Valerio, P. P. (2018), *Avaliação da difusão de íons cloreto considerando concreto simples constituído por três principais classes de cimento portland convencional.* Sodebras Journal. 13(151): 99-113. doi: https://doi.org/10.13140/RG.2.2.12429.64486

Godinho, J. P., Oliveira, R. L. N., Capraro, A. P. B., Réus, G. C., Medeiros, M. H. F. (2018), *"Influência das condições de limpeza de barras de aço carbono do concreto armado nas leituras eletroquímicas de densidade de corrente de corrosão e potencial de corrosão"*, in: Anais do 3º Encontro Luso-Brasileiro de Degradação em Estruturas de Concreto (3º DEGRADA), São Carlos/SP, 77–92.

Godinho, J. P., Zermiani, B. N., Oliveira, R. L. N., Medeiros, M. H. F. (2019), *Comportamento eletroquímico do aço carbono inserido no concreto durante a passivação*. Revista Técnico-Científica do CREA-PR. ISSN 2358-5420 –Edição Especial – Setembro de 2019, 1 - 16.

Gurdián, H.; García-Alcocel, E.; Baeza-Brotons, F.; Garcés, P.; Zornoza, E. (2014), *Corrosion behavior of steel reinforcement in concrete with recycled aggregates, fly ash and spent cracking catalyst.* Materials (Basel). 7(4), 3176-3197. doi: https://doi.org/10.3390/ma7043176

Gentil, V. (1996), "*Corrosão*". 3a Edição. Rio de Janeiro. Editora LTC. Capítulo 3: "Potencial de eletrodo". p 14 – 28.

Ghods, P., Isgor, O. B., McRae, G. A., Gub, G. P. (2010), *Electrochemical investigation of chloride-induced depassivation of black Steel rebar under simulated service conditions.* Corrosion Science. 52(5): 1649–1659. doi: https://doi.org/10.1016/j.corsci.2010.02.016

Ghods, P., Isgor, O. B., McRae, G., Miller, T. (2009), *The effect of concrete pore solution composition on the quality of passive oxide films on black steel reinforcement.* Cement and Concrete Composites. 31(1): 2–11. doi: https://doi.org/10.1016/j.cemconcomp.2008.10.003

Hays, G. F. (2020), *Now is the Time.* Director General da World Corrosion Organization. Acesso em: dezembro de 2020. Disponível em: http://corrosion.org/Corrosion+Resources/Publications/_/nowisthetime.pdf

Pei, H., Li, Z., Zhang, J., Wang, Q. (2015), *Performance investigations of reinforced magnesium phosphate concrete beams under accelerated corrosion conditions by multi techniques.* Construction Building Materials. 93: 982-994. https://doi.org/10.1016/j.conbuildmat.2015.05.057

Hernández, Y., Troconis de Rincón, O., Torres, A., Delgado, S., Rodríguez, J., Morón, O. (2016). *Relación entre la velocidad de corrosión de la armadura y el ancho de fisuras en vigas de concreto armado expuestas a ambientes que simulan el medio marino.* Revista ALCONPAT, 6(3), 272 - 283. https://doi.org/10.21041/ra.v6i3.152

Institut Für Seltene Erden und Strategische Metalle (ISE) (2020), *Preços, ocorrência, extração e uso do Titan*. Acesso em: dezembro de 2020. Disponível em: https://pt.institut-seltene-erden.de/seltene-erden-und-metalle/strategische-metalle-2/titan/

Inaudi, D. (2009), *"Integrated Structural Health Monitoring Systems for Bridges"*. in: Anais do 1o Congresso de Segurança e Conservação de Pontes ASCP'09. Lisboa. 2009.

Jucá, T. R. P. (2002), *"Avaliação de Cloretos Livres em Concretos e Argamassas de Cimento Portland pelo Método de Aspersão de Nitrato de Prata"*. Universidade Federal de Goiás. Escola Engenharia Civil II.

Jin, M., Jiang, L., Zhu, Q. (2017), *Monitoring chloride ion penetration in concrete with different mineral admixtures based on embedded chloride ion selective electrodes.* Construction Building Materials. 143: 1-5. 15 julho, 2017. https://doi.org/10.1016/j.conbuildmat.2017.03.131

Jiang, J. -Y., Wang, D., Chu, H. -Y., Ma, H., Liu, Y., Gao, Y., Shi, J., Sun, W. (2017), *The passive film growth mechanism of new corrosion-resistant steel rebar in simulated concrete pore solution: Nanometer structure and electrochemical study.* Materials (Basel). 10(4): 412. doi: https://doi.org/10.3390/ma10040412

Klassen, R. D., Roberge, P. R. (2008), *"Technique for corrosion monitoring"*. Capítulo 5: Zero resistance ammetry and galvanic sensor. p 111-124.
Leek, D. S. (1991), *The Passivity of Steel in Concrete.* Quarterly Journal of Engineering Geology. 24:55–66. https://doi.org/10.1144/GSL.QJEG.1991.024.01.05
Lv, H., Zhao, X., Zhan, Y., Gong, P. (2017), *Damage evaluation of concrete based on Brillouin corrosion expansion sensor*, Construction and Building Materials, 143: 387-394, ISSN 0950-0618, https://doi.org/10.1016/j.conbuildmat.2017.03.122
Mccarter, W. J., Vennesland, Ø. (2004), *Sensor systems for use in reinforced concrete structures.* Construction and Building Materials. 18(6): 351–358. https://doi.org/10.1016/j.conbuildmat.2004.03.008
Medeiros, M. H. F. (2008), *"Contribuição ao estudo da durabilidade de concretos com proteção superficial frente a ação de íons cloretos"*. Universidade de São Paulo. Escola Politécnica. 2008.
Medeiros, M. H. F., de Oliveira Andrade, J. J., Helene, P. (2011), *"Durabilidade e Vida Útil das Estruturas de Concreto"*. Capítulo 22, Concreto: Ciência e Tecnologia, Geraldo Cechella Isaia (Editor), © 2011 IBRACON. URL: http://www.phd.eng.br/wp-content/uploads/2014/07/lc55.pdf
Medeiros, M. H. F., Rocha, F. C., Medeiros-Junior, R. A., Helene, P. (2017), *Corrosion potential: influence of moisture, water-cement ratio, chloride content and concrete cover*, Revista IBRACON de Estruturas e Materiais (RIEM). 10 (4):864–885. https://doi.org/10.1590/s1983-41952017000400005
Torres-Luque, M., Bastidas-Arteaga, E., Schoefs, F., Sánchez Silva, M., Osma, J. F. (2014), *Non-destructive methods for measuring chloride ingress into concrete: State-of-the-art and future challenges.* Construction and Building Materials. 68:68-81. https://doi.org/10.1016/j.conbuildmat.2014.06.009
Marcondes, C. G. N. (2012), *"Adição de nanotubos de carbono em concretos de cimento Portland absorção, permeabilidade, penetração de cloretos e propriedades mecânicas"*. Universidade Federal do Paraná. Setor de Tecnologia. Programa de Pós-Graduação em Engenharia de Construção Civil – PPGECC. 2012.
Meira, G. R. (2017), *"Corrosão de Armaduras em Estruturas de Concreto - fundamentos, diagnóstico e prevenção"*. 1ª edição, editora do IFPB, João Pessoa-PB, 2017.
Macioski, G., de Souza, D. J., Capraro Brandão, A. P., de Medeiros, M. H. F. (2016). *Análisis de la corrosión de barras de acero en función de la variación del pH del medio.* Revista ALCONPAT, 6(3), 223 - 234. https://doi.org/10.21041/ra.v6i3.153
Mota, A. C. M. (2011), *"Avaliação da presença de cloretos livres em argamassas através do método colorimétrico de aspersão da solução de nitrato de prata"*. Dissertação de mestrado. Escola Politécnica da Universidade de Pernambuco, Recife, Brasil.
Martínez, I., Andrade, C. (2009), *Examples of reinforcement corrosion monitoring by embedded sensors in concrete structures.* Cement and Concrete Composites, 31(8): 545–554. doi: https://doi.org/10.1016/j.cemconcomp.2009.05.007
Nahali, H., Dhouibi, L., Idrissi, H. (2014), *Effect of phosphate based inhibitor on the threshold chloride to initiate steel corrosion in saturated hydroxide solution.* Construction and Building Materials. 50: 87–94. https://doi.org/10.1016/j.conbuildmat.2013.08.054
Pérez López, T., Sosa, M. R., Moo-Yam, V. M. J., Chávez, E., Pérez-Quiroz, J. T. (2018). *Análisis de la interfaz concreto-acero en especímenes expuestos a la intemperie e inmersos en agua de mar natural.* Revista ALCONPAT, 8(1), 16 - 29. https://doi.org/10.21041/ra.v8i1.203
Pereira, E. V., Salta, M. M. (2012), *"Monitorização permanente da corrosão em estruturas de betão armado". Resultados a longo prazo"*, in: Anais do Encontro Nacional BETÃO ESTRUTURAL - BE2012. FEUP, 24-26 de octubro de 2012.

Pereira, E. V., Figueira, R. B., Salta, M. M. L., Da Fonseca, I. T. E. (2009), *A Galvanic Sensor for Monitoring the Corrosion Condition of the Concrete Reinforcing Steel: Relationship Between the Galvanic and the Corrosion Currents.* Journal of Sensor. 9(11): 8391-8398. doi: https://doi.org/10.3390/s91108391; ISSN 1424-8220. 2009.

Pawlick, L. A., Stoner, G. E., Clemeña, G. G. (1998), *Development of an embeddable reference electrode for reinforced concrete structures.* Contract Research Sponsored by Virginia Transportation Research Council. URL: https://www.virginiadot.org/vtrc/main/online_reports/pdf/99-cr1.pdf

Park, Z.-T., Choi, Y.-S., Kim, J.-G., Chung, L. (2005), *Development of a galvanic sensor system for detecting the corrosion damage of the steel embedded in concrete structure. Part 2. Laboratory electrochemical testing of sensors in concrete.* Cement and Concrete Research. 35(9): 1814 –1819. https://doi.org/10.1016/j.cemconres.2003.11.027

Pontes, C. V., Réus, G. C., Araújo, E.C., Medeiros, M. H. F. (2020), *Silver nitrate colorimetric method to detect chloride penetration in carbonated concrete: How to prevent false positives.* Journal of Building Engineering. (34): 101860. https://doi.org/10.1016/j.jobe.2020.101860

Poursaee, A. (2016), *Corrosion of Steel in Concrete Structures.* Elsevier, 1st Edition. Amsterdã, Holanda, 2016.

Pereira, V. G. A. (2001), *"Avaliação do coeficiente de difusão de cloretos em concretos: influência do tipo de cimento, da relação a/c, da temperatura e do tempo de cura"*. Dissertação de mestrado Programa de Pós-Graduação em Engenharia Civil Universidade Federal de Rio Grande do Sul.

Real, L. V., Oliveira, D. R. B., Soares, T., Medeiros, M. H. F. (2015). *Método colorimétrico por aspersión de nitrato de plata para la evaluación de la penetración de cloruros en concreto: estado del arte.* Revista ALCONPAT, 5(2), 149 - 159. https://doi.org/10.21041/ra.v5i2.84

Romano, P., Brito, P. S. D., Rodrigues, L. (2013), *Monitoring of the degradation of concrete structures in environments containing chloride ions.* Construction and Building Materials. 47: 827–832. https://doi.org/10.1016/j.conbuildmat.2013.05.042

Ribeiro, V. D., Cunha, T. M. P. (2014), *"Corrosão em Estructuras de Concreto Armado"*. Capítulo 8: Técnicas de avaliação e monitoramento da corrosão em estructuras de concreto armado, p 215.

Ribeiro, D. V., Helene, P., Cascudo, O., Tutikian, B. F., Sales, A., Souza, C. A. C., Cunha, M. P. T., Lourenco, M. Z., Almeida, F. C. R. (2018), *"Corrosão e Degradação em Estruturas de Concreto: Teoria, Controle e Técnicas de Análise e Intervenção"*. 2a, Elsevier Brasil, Rio de Janeiro-RJ, 2018.

Rocha, F. C. (2012), *"Leituras de potencial de corrosão em estruturas de concreto armado: influência da relação água / cimento, da temperatura, da contaminação por cloretos, da espessura de cobrimento e do teor de umidade do concreto"*. Dissertação de mestrado. Programa de Pós-graduação em engenharia de construção civil – PPGECC. Universidade Federal do Paraná. Curitiba 2012.

Rocha, F., Campos, H., de Andrade, T. S., Roquitski, A., Medeiros, M. H. (2014). *Influência da espessura de cobrimento e da contaminação por cloretos nas leituras de potencial de corrosão de armaduras.* REEC - Revista Eletrônica De Engenharia Civil, 8(2). https://doi.org/10.5216/reec.v8i2.26968

Raupach M., Schießl, P. (2001), *Macrocell sensor systems for monitoring of the corrosion risk of the reinforcement in concrete structures.* NDT & E International. 34(6): 435-442. https://doi.org/10.1016/S0963-8695(01)00011-1

Ribeiro, D. V., Souza, C. A. C., Abrantes, J. C. C. (2015), *Uso da Espectroscopia de Impedância Eletroquímica (EIE) para monitoramento da corrosão em concreto armado.* Revista IBRACON de Estruturas e Materiais. 8 (4): 529-546. Agosto 2015. https://doi.org/10.1590/S1983-41952015000400007

Sousa, C. D. C. A. (2014), *"Corrosão em estruturas de concreto armado: Teoria, Controle e Métodos de Análise"*. Capítulo 2: Princípios da corrosão eletroquímica., p 13-34.
Silva, P. N. R. (2017), *Ataque em estruturas de concreto por ação de cloretos.* Acesso em: dezembro 2017. Disponível em: https://www.axfiber.com.br/single-post/2017/01/12/ataque-em-estruturas-de-concreto-por-a%C3%A7%C3%A3o-de-cloretos
Silva, E. P. (2010), *"Avaliação do potencial de corrosão de concretos estruturais produzidos segundo as prescrições da NBR 6118, submetido a ensaio de corrosão acelerado"*. Dissertação (Graduação) -Curso de Engenharia Estrutural e Construção Civil de Fortaleza. Universidade Federal do Ceará. Fortaleza 2010.
Santos, L. O. (2014), *"Monitoramento e ensaio de Pontes"*. in: Anais do Congresso Brasileiro de Pontes e Estruturas. Rio de Janeiro. p 1-14. 21-23 de Maio del 2014.
Wu, L., Li, W., Yu, X. (2017), *Time-dependent chloride penetration in concrete in marine environments.* Construction and Building Materials. 152: 406-413. https://doi.org/10.1016/j.conbuildmat.2017.07.016
Williamsona, J., Isgor, O. B. (2016), *The effect of simulated concrete pore solution composition andchlorides on the electronic properties of passive films on carbon steelrebar.* Corrosion Science. 106: 82–95. http://dx.doi.org/10.1016/j.corsci.2016.01.027
Zhang, J., Lui, C., Sun, M., Li, Z. (2017). *An innovative corrosion evaluation technique for reinforced concrete structures using magnetic sensors.* Construction and Building Materials. 135: 68-75. http://dx.doi.org/10.1016/j.conbuildmat.2016.12.157
Zoghi, M. (2013), *"The International Handbook of FRP composites in civil engineering"*. 1st Edition. CRC Press. ISBN 9780849320132. September 26, 2013. Acesso: Janeiro, 2016. Disponível em: https://www.crcpress.com/TheInternational-Handbook-of-FRP-CompositesinCivilEngineering/Zoghi/p/book/9780849320132